J|A|C|S ARTICLES

Published on Web 06/11/2009

Real-Time Monitoring of Cell-Free Translation on a Quartz-Crystal Microbalance

Shuntaro Takahashi,[†,‡] Masaaki Iida,[†] Hiroyuki Furusawa,[†] Yoshihiro Shimizu,[§] Takuya Ueda,[§] and Yoshio Okahata*[,†]

Department of Biomolecular Engineering and Global Center of Excellence Program, Tokyo Institute of Technology, B-53, 4259 Nagatsuta, Midori-ku, Yokohama 226-8501, Japan, JST-SENTAN and Department of Medical Genome Sciences, Graduate School of Frontier Sciences, University of Tokyo, FSB401, 5-1-5 Kashiwanoha, Kashiwa, Chiba 277-8562, Japan

Received March 14, 2009; E-mail: yokahata@bio.titech.ac.jp

Abstract: The efficiency of protein synthesis is often regulated post-transcriptionally by sequences within the mRNA. To investigate the reactions of protein translation, we established a system that allowed real-time monitoring of protein synthesis using a cell-free translation mixture and a 27 MHz quartz-crystal microbalance (QCM). Using an mRNA that encoded a fusion polypeptide comprising the streptavidin-binding peptide (SBP) tag, a portion of Protein D as a spacer, and the SecM arrest sequence, we could follow the binding of the SBP tag, while it was displayed on the 70S ribosome, to a streptavidin-modified QCM over time. Thus, we could follow a single turnover of protein synthesis as a change in mass. This approach allowed us to evaluate the effects of different antibiotics and mRNA sequences on the different steps of translation. From the results of this study, we have determined that both the formation of the initiation complex from the 70S ribosome, mRNA, and fMet−tRNA^{fMet} and the accommodation of the second aminoacyl-tRNA to the initiation complex are rate-limiting steps in protein synthesis.

Introduction

Proteins are synthesized by ribosomes, which decode the genetic information within mRNAs that have been transcribed from DNA. Many factors interact with the ribosome during protein synthesis, even in bacteria, to enable the sophisticated reactions of translation to occur.[1−3] The translation process in bacteria is divided into three steps. First, a bacterial ribosome binds to the Shine−Dalgarno (SD) sequence on an mRNA to form an initiation complex (translation initiation). Second, the ribosome catalyzes the polymerization of amino acids to form a polypeptide chain, whose sequence is determined by the genetic information within the mRNA (translation elongation). Third, the completed polypeptide chain is released and the ribosome is recycled (translation termination). Although protein expression is determined predominantly by the amount of mRNA that is transcribed,[4] it can also be regulated at the post-transcriptional level by noncoding sequences within individual mRNAs, such as translational enhancers within the 5′ untranslated region (5′-UTR)[5−7] or riboswitches, which regulate translational initiation after binding specific metabolites.[8−10] Moreover, it has been reported that silent polymorphisms could affect the activity of the synthesized protein by altering the rate of translation, which in turn affects the folding of the protein.[11−13] Thus, the mRNA sequence does not just contain the genetic information but can also regulate the activity of ribosomes during translation initiation and elongation. To evaluate the translational efficiency of a specific mRNA from the formation of the initiation complex until translation termination, a series of single-turnover translation reactions must be observed in real time.

Translation can be accomplished in vitro using a cell-free extract or reconstituted *Escherichia coli* translational factors (the PURE system).[14−16] The primary method for quantitation of the product of a single-turnover translation reaction involves labeling of the product with a radioactive isotope. However, this approach is not suitable for observations in real time.[16] Recently, some single-molecule imaging techniques have been

[†] Department of Biomolecular Engineering, Tokyo Institute of Technology.
[‡] Global Center of Excellence Program, Tokyo Institute of Technology.
[§] University of Tokyo.

(1) Wintermeyer, W.; Peske, F.; Beringer, M.; Gromadski, K. B.; Savelsbergh, A.; Rodnina, M. V. *Biochem. Soc. Trans.* **2004**, *32*, 733–737.
(2) Laursen, B. S.; Sørensen, H. P.; Mortensen, K. K.; Sperling-Petersen, H. U. *Microbiol. Mol. Biol. Rev.* **2005**, *69*, 101–123.
(3) Steitz, T. A. *Nat. Rev. Mol. Cell Biol.* **2008**, *9*, 242–253.
(4) Beckwith, J. In *Escherichia coli and Salmonella: Cellular and Molecular Biology*, 2nd ed.; ASM Press: Washington, DC, 1996; Chapter 78, pp 1227−1231.
(5) Olins, P. O.; Devine, C. S.; Rangwala, S. H.; Kavka, K. S. *Gene* **1988**, *73*, 227–235.
(6) Olins, P. O.; Rangwala, S. H. *J. Biol. Chem.* **1989**, *264*, 16973–16976.
(7) Komarova, A. V.; Tchufistova, L. S.; Supina, E. V.; Boni, I. V. *RNA* **2002**, *8*, 1137–1147.
(8) Winkler, W.; Nahvi, A.; Breaker, R. R. *Nature* **2002**, *419*, 952–956.
(9) Barrick, J. E.; Corbino, K. A.; Winkler, W. C.; Nahvi, A.; Mandal, M.; Collins, J.; Lee, M.; Roth, A.; Sudarsan, N.; Jona, I.; Wickiser, J. K.; Breaker, R. R. *Proc. Natl. Acad. Sci. U.S.A.* **2004**, *101*, 6421–6426.
(10) Bayer, T. S.; Smolke, C. D. *Nat. Biotechnol.* **2005**, *23*, 337–343.
(11) Komar, A. A.; Lesnik, T.; Reiss, C. *FEBS Lett.* **1999**, *462*, 387–391.
(12) Kimchi-Sarfaty, C.; Oh, J. M.; Kim, I. W.; Sauna, Z. E.; Calcagno, A. M.; Ambudkar, S. V.; Gottesman, M. M. *Science* **2007**, *315*, 525–528.
(13) Iskakova, M. B.; Szaflarski, W.; Dreyfus, M.; Remme, J.; Nierhaus, K. H. *Nucleic Acids Res.* **2006**, *34*, e135.

 10.1021/ja9019947 CCC: $40.75

applied to the observation of protein synthesis; they utilize specialized templates or fluorescent proteins.[17−19] Therefore, there are currently only a few available methods that can be used to measure and evaluate the reactions of protein synthesis in real time with intact molecules.

Here we report the real-time monitoring of a cell-free, single-turnover translation reaction on a 27 MHz quartz-crystal microbalance (QCM) with no labeling. A QCM can measure increases in mass on its surface at the nanogram level by detecting decreases in frequency in the solution. We applied the QCM technique to the enzymatic reactions of DNA polymerase and endonuclease to investigate the mechanism of these enzymatic reactions.[20−24] The PURE system (a reconstituted cell-free system) is a useful tool for the elucidation of the translation machinery because the recombinant components can be adjusted easily.[15,16,26,27] Cell-free translations were started by the addition of an mRNA that encoded the streptavidin-binding peptide (SBP) tag, Protein D as a spacer, and the SecM arrest sequence to a streptavidin-modified QCM cell that contained the *E. coli* translation reaction mixture. We monitored the decreases in frequency (i.e., increases in mass) that occurred on the QCM due to the binding of the SBP tag, which was displayed by the 70S ribosome bound to the mRNA. Thus, we could follow a single-turnover translation reaction as a change in mass. In addition, we studied the effects of different antibiotics and 5′-UTRs on the translation rate.

Experimental Section

Materials. 1-Ethyl-3-[(3-dimethylamino)propyl]carbodiimide (EDC) was purchased from Dojindo Laboratories (Kumamoto, Japan), and *N*-hydroxysuccinimide (NHS) and streptavidin were purchased from Wako Pure Chemical Industries, Ltd. (Osaka, Japan). The oligonucleotides were purchased from Operon (Tokyo, Japan). Lipidure-BL405 was obtained from NOF (Tokyo, Japan). All other materials were purchased from Nacalai Tesque (Kyoto, Japan) and used without further purification.

Factors for Cell-Free Translation. *E. coli* 70S ribosomes, initiation factors (IFs) IF1−3, elongation factors (EFs) EF-Tu, EF-G, and EF-Ts, and methionyl tRNA formyltransferase (MTF) were prepared and purified as described previously.[15,27] The 20 aminoacyl−tRNA synthetases and the energy recycling system were prepared and mixed as described elsewhere.[26] The guanosine diphosphate in EF-Tu was exchanged for guanosine triphosphate (GTP) by pretreating 250 μM purified EF-Tu with 1 mM GTP, 2.4 units mL^{-1} pyruvate kinase, and 3 mM phosphoenol pyruvate. The template DNA, which encoded a fusion protein consisting of the SBP tag[28] [MDEKTTGWRGGHVVEGLAGELEQLRARLEHH-PQGQGREP, 38 amino acids (aa)], a portion of Protein D as a spacer (MGTATAPGGLSAKAPAMTPLMLDTSSRKLVAWD-GTTDGAAVGILAVAADQTSTTLTFYKSGTFRYEDVLWPEA-ASDETKKRTAFAGTAISIV, 92 aa), and the SecM arrest sequence (TPVWISQAQGIRAGPQRLT, 23 aa), was cloned downstream of a T7 promoter[27] and various 5′-UTR sequences. Translation of the resulting mRNA produced a ribosome complex that displayed the SBP tag (see Figure 1A). The 5′-UTR sequences that were employed in this study (Can-mRNA, Strong-mRNA, and Enhancer-mRNA) are summarized in Table 1. The template DNAs were amplified by PCR, after which mRNA was transcribed using T7 RNA polymerase (Takara, Shiga, Japan) and purified with MicroSpin G-25 columns (GE Healthcare, Buckinghamshire, England). We also prepared mRNA that encoded a T7 tag (MASMGGQQMG, 10 aa) instead of an SBP tag, with the remaining coding sequence identical to that of the SBP-encoding mRNA.

Setup of the Streptavidin-Modified 27 MHz QCM. An AFFINIX Q4 system with four 500 μL cells together with a stirring bar and a temperature control system (see Figure 1B) was used as the QCM apparatus (Initium Co., Ltd., Tokyo, Japan). Each cell was equipped with a 27 MHz QCM plate oscillating at a fundamental frequency (8.7 mm diameter quartz plate and 5.7 mm^2 gold electrode) on the bottom of the cell. Sauerbrey's equation (eq 1) was obtained for an AT-cut shear mode QCM in the air phase:

$$\Delta F_{\mathrm{air}} = -\frac{2F_0^{\,2}}{A\sqrt{\rho_{\mathrm{q}}\mu_{\mathrm{q}}}}\Delta m \qquad (1)$$

where ΔF_{air} is the measured frequency change in the air phase (Hz), F_0 is the fundamental frequency of the quartz crystal prior to the mass change (27×10^6 Hz), Δm is the mass change (g), A is the electrode area (0.057 cm^2), ρ_{q} is the density of quartz (2.65 g cm^{-3}), and μ_{q} is the shear modulus of quartz (2.95×10^{11} dyn cm^{-2}). In the air phase, a 0.62 ng cm^{-2} mass increase for each 1 Hz decrease in frequency was obtained from previous experiments;[20−25] this agreed well with the value of 0.61 ng cm^{-1} Hz^{-1} calculated numerically from eq 1. However, when the QCM is employed in an aqueous solution, one must also consider the effects of hydration and/or viscoelasticity of the biomolecules. This can be done by inserting a correction factor, $\Delta F_{\mathrm{water}}/\Delta F_{\mathrm{air}}$, into eq 1 to obtain eq 2:

$$\Delta F_{\mathrm{water}} = -\frac{\Delta F_{\mathrm{water}}}{\Delta F_{\mathrm{air}}}\frac{2F_0^{\,2}}{A\sqrt{\rho_{\mathrm{q}}\mu_{\mathrm{q}}}}\Delta m \qquad (2)$$

We therefore directly calibrated the relationship between $\Delta F_{\mathrm{water}}$ and ΔF_{air} for a ribosome binding onto a QCM plate. There was a good linear correlation between $\Delta F_{\mathrm{water}}$ and ΔF_{air}, with a slope of 3.3 ± 0.2, for binding of the 70S ribosome. Thus, frequency decreases in water ($\Delta F_{\mathrm{water}}$) due to the ribosome bindings were 3.3 times larger than those in the air phase (ΔF_{air}) because hydrating water vibrates along with large ribosomes. Therefore, the $\Delta F_{\mathrm{water}}/\Delta F_{\mathrm{air}}$ value for this ribosome was determined to be 3.3 ± 0.2, and the factor relating $\Delta m/A$ to $-\Delta F_{\mathrm{water}}$ in Sauerbrey's equation for ribosomes in aqueous solutions (eq 2) was obtained as (0.62 ng cm^{-2} Hz^{-1})/3.3 = 0.19 ± 0.02 ng cm^{-2} Hz^{-1}.

The noise level of the 27 MHz QCM was ±1 Hz in buffer solutions at 25 °C, and the standard deviation of the frequency was ±2 Hz for a 1 h immersion in buffer solution at 25 °C. The sensitivity of 0.19 ng cm^{-2} Hz^{-1} was sufficiently large to sense

(14) Kim, D. M.; Swartz, J. R. *Biotechnol. Prog.* **2000**, *16*, 385–390.
(15) Shimizu, Y.; Inoue, A.; Tomari, Y.; Suzuki, T.; Yokogawa, T.; Nishikawa, K.; Ueda, T. *Nat. Biotechnol.* **2001**, *19*, 751–755.
(16) Udagawa, T.; Shimizu, Y.; Ueda, T. *J. Biol. Chem.* **2004**, *279*, 8539–8546.
(17) Wen, J. D.; Lancaster, L.; Hodges, C.; Zeri, A. C.; Yoshimura, S. H.; Noller, H. F.; Bustamante, C.; Tinoco, I. *Nature* **2008**, *452*, 598–603.
(18) Uemura, S.; Iizuka, R.; Ueno, T.; Shimizu, Y.; Taguchi, H.; Ueda, T.; Puglisi, J. D.; Funatsu, T. *Nucleic Acids Res.* **2008**, *36*, e70.
(19) Ellis, J. P.; Bakke, C. K.; Kirchdoerfer, R. N.; Jungbauer, L. M.; Cavagnero, S. *ACS Chem. Biol.* **2008**, *3*, 555–566.
(20) Matsuno, H.; Niikura, K.; Okahata, Y. *Chem.−Eur. J.* **2001**, *7*, 3305–3312.
(21) Matsuno, H.; Niikura, K.; Okahata, Y. *Biochemistry* **2001**, *40*, 3615–3622.
(22) Matsuno, H.; Furusawa, H.; Okahata, Y. *Biochemistry* **2005**, *44*, 2262–2270.
(23) Takahashi, S.; Matsuno, H.; Furusawa, H.; Okahata, Y. *Anal. Biochem.* **2007**, *361*, 210–217.
(24) Takahashi, S.; Matsuno, H.; Furusawa, H.; Okahata, Y. *J. Biol. Chem.* **2008**, *283*, 15023–15030.
(25) (a) Takahashi, S.; Akita, R.; Matsuno, H.; Furusawa, H.; Shimizu, Y.; Ueda, T.; Okahata, Y. *ChemBioChem* **2008**, *9*, 870–873. (b) Furusawa, H.; Ozeki, T.; Morita, M.; Okahata, Y. *Anal. Chem.* **2009**, *81*, 2268–2273.
(26) Shimizu, Y.; Kanamori, T.; Ueda, T. *Methods* **2005**, *36*, 299–304.
(27) Ohashi, H.; Shimizu, Y.; Ying, B. W.; Ueda, T. *Biochem. Biophys. Res. Commun.* **2007**, *352*, 270–276.
(28) Keefe, A. D.; Wilson, D. S.; Seelig, B.; Szostak, J. W. *Protein Expression Purif.* **2001**, *23*, 440–446.

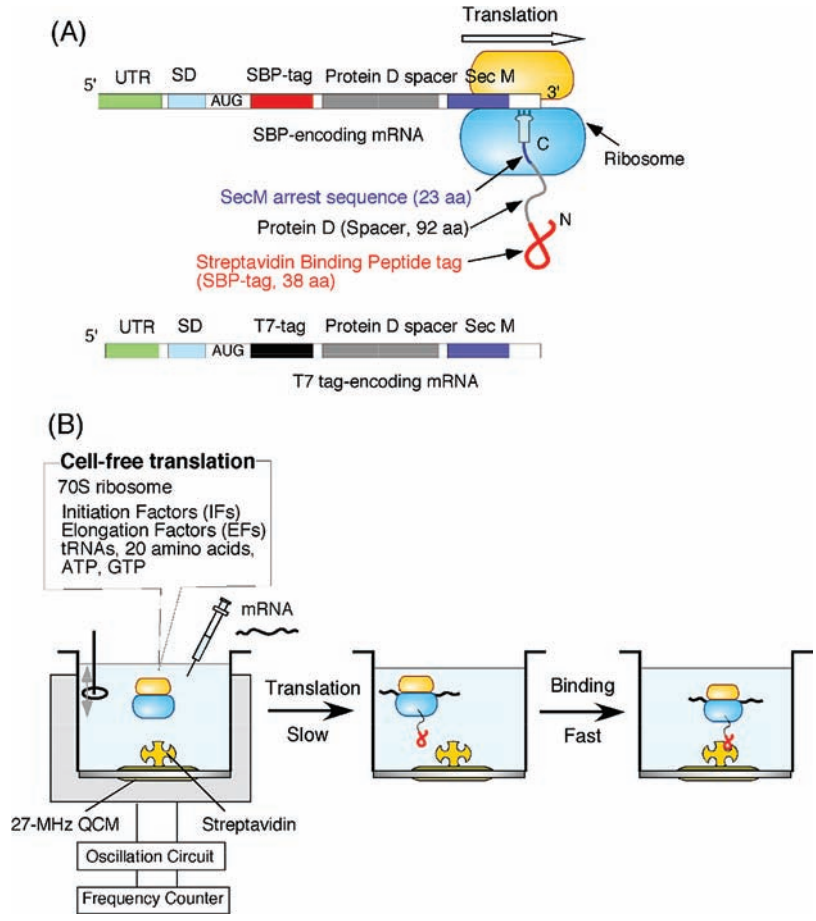

Figure 1. Schematic illustrations of (A) the 70S ribosome nascent chain complex (RNC) presenting the SBP or T7 tag and (B) trapping of the SBP tag of the RNC on a streptavidin-modified 27 MHz QCM triggered by the addition of mRNA.

Table 1. Sequences of the 5′-UTRs of the mRNAs[a]

mRNA	Sequence (5' → 3')
Can-mRNA	5'-gggagaccacaacggguuucccucuagaaauaauuuugu-cauggauucagAAGGAGauauacauaug–
Strong-mRNA	5'-gggagaccacaacggguuucccucuagaaauaauuuugu-cauggauucaUAAGGAGGTGATCaug–
Enhancer-mRNA	5'-gggagaccacaacggguuucccucuagaaauaauuuugu-UUAACUUUAAgAAGGAGauauacauaug–

[a] Regions that are complementary to the 16S rRNA (the anti-SD sequence) are underlined. Boxes indicate the start codon of the SBP fusion polypeptide.

the binding of ribosomes. The details of these calibration experiments were described previously.[25]

3,3-Dithiodipropionic acid was immobilized onto the cleaned bare gold electrode, and then the carboxyl groups were activated with NHS and EDC. The activated carboxyl groups were reacted with the amino groups of streptavidin in a QCM cell that had been filled with a buffer solution [10 mM HEPES (pH 7.6), 50 mM NaCl]. The maximum decrease in frequency was $\Delta F = -550 \pm 50$ Hz. From this value, the amount of immobilized streptavidin (MW = 64 kDa; ~6 × 6 × 4 nm) was calculated to be 140 ± 13 ng cm^{-2} (2.3 ± 0.2 pmol cm^{-2}) using the calibration of 0.26 ng cm^{-2} Hz^{-1}.[29] This amount corresponded to ~50% coverage of the QCM surface (4.5 pmol cm^{-2} would represent complete coverage of the QCM surface with streptavidin).

(29) Ozeki, T.; Morita, M.; Yoshimine, H.; Furusawa, H.; Okahata, Y. *Anal. Chem.* **2007**, *79*, 79–88.

Table 2. Components of the Translation Mixture in the QCM Cell (Total Volume 500 μL)[a]

substrates and chemicals	enzymes
20 amino acids at 20 μM	1.5 μM IF1
0.4 mM ATP, GTP	0.15 μM IF2
0.2 mM UTP, CTP	0.15 μM IF3
4 mM creatine phosphate	1.6 μM EF-Tu
2 μg mL^{-1} formyldonor	0.4 μM EF-Ts
11.2 OD mL^{-1} total tRNA from *E. coli*	0.8 μM EF-G
0.5 wt % Lipidure-BL405	2−20 units of ARS, MTF, energy mixture
buffer mixture[b]	40 nM *E. coli* 70S ribosomes 80 nM mRNA

[a] 70S ribosomes were treated in an enzyme mixture prior to the experiment. The enzyme mixture contained all the substrates and chemicals, each factor at a 5× concentration, and 0.4 μM 70S ribosome in buffer mixture without Lipidure-BL405. Abbreviations: ATP, adenosine triphosphate; GTP, guanosine triphosphate; UTP, uridine triphosphate; CTP, cytidine triphosphate; IF, initiation factor; EF, elongation factor; ARS, aminoacyl−tRNA synthetase; formyldonor, 10-formyl-5,6,7,8-tetrahydrofolic acid; energy mixture, see ref 26; MTF, methionyl tRNA formyl transferase. [b] Buffer mixture contents: 50 mM HEPES-KOH (pH 7.6), 100 mM potassium glutamate, 13 mM $Mg(OAc)_2$, 2 mM spermidine, 1 mM DTT.

Translation on the QCM. The translation reaction mixture was prepared as shown in Table 2. Prior to the measurements, 50 μL of enzyme mixture, which contained the 70S ribosomes, IFs, EFs, aminoacyl−tRNA synthetases, and MTF, was incubated at 37 °C for 5 min as a preincubation. The enzyme mixture was then added to 450 μL of the reaction mixture, which contained all of the enzymes except the ribosomes together with the substrates and

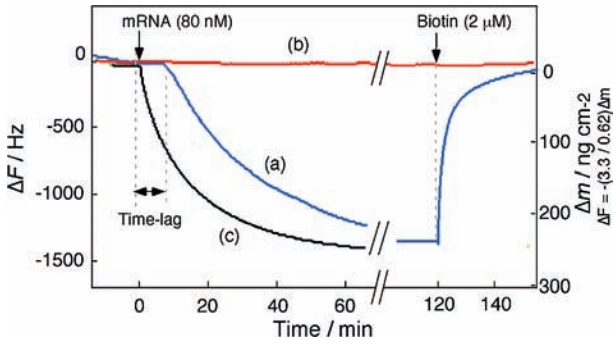

Figure 2. Typical frequency decreases (mass increases) in the streptavidin-modified 27 MHz QCM cell filled with *E. coli* cell-free translation mixture in response to the addition of (a) SBP-tag-encoding mRNA, (b) T7-tag-encoding mRNA, or (c) preformed RNCs presenting the SBP tag. Conditions: 50 mM HEPES buffer (pH 7.6), 40 nM ribosomes, 80 nM mRNA, 25 °C. The other components of the translation reaction mixture are summarized in Table 2.

chemicals, in the QCM cell (500 μL volume) in the AFFINIX Q4 apparatus at 25 °C. After the frequency became constant (within $\pm$2 Hz), the solution of mRNA was injected to start the translation. The reaction mixture was stirred vigorously to avoid any anomalies due to lack of mixing, and the decreases in frequency (increases in mass) were followed over time. When the translation reaction was complete, the ribosome nascent chain complexes (RNCs) that had been produced were collected by ultracentrifugation and used as preformed RNCs. To trigger protein synthesis by the addition of an EF, EF-Tu or EF-G was omitted from the reaction solution initially, and then 1.6 μM EF-Tu/GTP or 0.8 μM EF-G, respectively, was added to the reaction solution 20 min after the mRNA was injected.

Analysis of Translation Initiation. The frequency of the solution decreased linearly during the first 20−30 min of the reaction as a result of trapping of the ribosome-displayed SBP. The normalized decreases in frequency were subjected to a smoothing process and converted to their derivative plots to find their linearity using KaleidaGraph (Synergy Software, Reading, PA). The frequency changes were fitted by regression analysis, and the point of intersection with the time axis was determined to define the efficiency of translation initiation as a time lag.

Results and Discussion

To trap the nascent peptide that is displayed on ribosomes during cell-free translation, we designed an open reading frame (ORF) that encoded the SBP tag (38 aa) followed by a portion of Protein D as a spacer (92 aa) and the SecM arrest sequence (23 aa). This ORF was ligated to different 5′-UTRs and an SD sequence. Ninety-two amino acids of Protein D were utilized because this length allowed the SBP tag to be freely available for binding when the SecM arrest sequence was trapped in the tunnel of the 50S ribosomal subunit.[30] As a control, we also prepared mRNAs that encoded a T7 tag (10 aa) instead of an SBP tag. With the exception of the tag sequences, the SBP- and T7-tag-encoding mRNAs were identical. It was expected that as soon as the SBP tag was available on the 70S ribosome, it would become trapped on the streptavidin-modified QCM because of the strong interaction between SBP and streptavidin ($K_d = 10^{-9}$ M).[31]

Curve (a) in Figure 2 shows a typical decrease in frequency as a function of time after the injection of SBP-tag-encoding mRNA (Can-mRNA) into a QCM cell that contained the *E. coli* cell-free translation mixture. After a time lag of ~10 min, the frequency decreased gradually (as the mass increased) and finally reached a constant value of $-\Delta F = 1200 \pm 200$ Hz ($\Delta m = 240 \pm 40$ ng cm^{-2}). When biotin, whose affinity for streptavidin ($K_d = 10^{-15}$ M) is much greater than that of the SBP tag ($K_d = 10^{-9}$ M), was added after equilibrium had been reached, the frequency began to increase rapidly (as the mass on the balance decreased) and reverted almost to the original value. The RNCs that were produced in the bulk solution were collected by ultracentrifugation and injected at the same concentration into a streptavidin-modified QCM cell. When the preformed RNCs were injected, the frequency decreased immediately with no time lag and reached the same level as that for the newly formed RNCs [curve (c)]. In contrast, the frequency was hardly affected by the addition of the mRNA that encoded the T7 tag, which did not bind streptavidin [curve (b)]. When a peptide that did not contain the Protein D spacer was synthesized, the decrease in frequency was small, which might be due to steric hindrance or unfolding of the SBP tag (data not shown).

The observed change in mass was 240 $\pm$ 40 ng cm^{-2}. The MW of the SBP fusion polypeptide was 19 kDa, which was considerably less than that of the ribosome (2520 kDa). We immobilized 170 $\pm$ 20 ng cm^{-2} (2.6 $\pm$ 0.2 pmol cm^{-2}) of streptavidin on the QCM plate (see the Experimental Section). If just one or two SBP-tag fusion peptides were bound to one streptavidin tetramer (two of the biotin-binding sites would be accessible from the bulk solution on the QCM surface), a mass increase of 50−100 ng cm^{-2} would be expected. Thus, the large increase in mass that was observed (240 $\pm$ 40 ng cm^{-2}) indicated that 0.1 pmol cm^{-2} of RNCs were generated in a single-turnover reaction in the presence of 40 nM ribosomes (20 pmol in 500 μL). Although the frequency decreased immediately and rapidly after the addition of preformed RNCs, when the SBP-tag-encoding mRNA was injected into the translation mixture, the decrease in frequency occurred gradually and after a time lag. This time lag represents the time required for the ribosome to synthesize the SBP tag, which includes the formation of the initiation complex and translational elongation. The slope of the frequency decrease reflected the rate of production of the ribosome-displayed SBP. In vivo, *E. coli* ribosomes can polymerize 10−20 amino acids per second in the presence of a relatively high concentration (>μM) of translation factors and substrates.[32] In our QCM experiments, we used very low concentrations of translation factors, particularly the IFs (0.5 μM), tRNAs (18 μM), and mRNA (80 nM), and the reaction was performed at a low temperature (25 °C). Under these conditions, ~1 h was required for the 153 aa peptide to be synthesized.

Effect of Antibiotics on Translation. In general, antibiotics function by inhibiting the action of ribosomes and preventing protein translation. Here we used puromycin, fusidic acid, and kasugamycin to evaluate the effects of these antibiotics on the translation reactions. Puromycin, which is an analogue of an aminoacyl−tRNA, binds in the A site of the ribosome and

(30) Nakatogawa, H.; Ito, K. *Cell* **2002**, *108*, 629–636.
(31) Wilson, D. S.; Keefe, A. D.; Szostak, J. W. *Proc. Natl. Acad. Sci. U.S.A.* **2001**, *98*, 3750–3755.
(32) Wilson, D. N.; Nierhaus, K. H. *Angew. Chem., Int. Ed.* **2003**, *42*, 3464–3486.
(33) Okuyama, A.; Machiyama, N.; Kinoshita, N.; Tanaka, N. *Biochem. Biophys. Res. Commun.* **1971**, *43*, 196–199.
(34) Schluenzen, F.; Takemoto, C.; Wilson, D. N.; Kaminishi, T.; Harms, J. M.; Hanawa-Suetsugu, K.; Szaflarski, W.; Kawazoe, M.; Shirouzu, M.; Nierhaus, K. H.; Yokoyama, S.; Fucini, P. *Nat. Struct. Mol. Biol.* **2006**, *13*, 871–878.

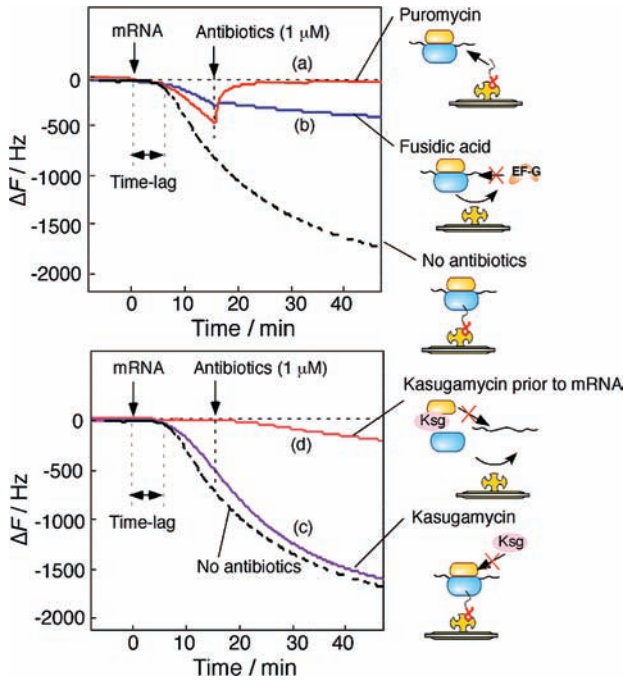

Figure 3. Typical frequency changes in the QCM in response to the addition of the antibiotics (a) puromycin, (b) fusidic acid, and (c) kasugamycin 15 min after the addition of mRNAs and (d) kasugamycin added prior to the addition of mRNA. The dotted lines show the frequency decrease in the absence of antibiotics. Conditions: 50 mM HEPES buffer (pH 7.6), 40 nM ribosomes, 80 nM mRNA, 1 μM antibiotics, 25 °C. The other components of the translation reaction mixture are summarized in Table 2.

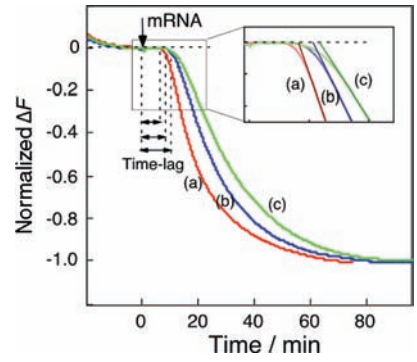

Figure 4. Effect of different 5′-UTR sequences on the time lag between the addition of mRNA and the start of translation: (a) Enhancer-mRNA (UUAACUUUAAgAAGGAG), (b) Can-mRNA (AAGGAG), and (c) Strong-mRNA (UAAGGAGGTGATC). The underlined SD sequence is complementary to the 16S rRNA of the 30S ribosome. The inset shows enlargements of the initial slopes. Conditions: 50 mM HEPES buffer (pH 7.6), 40 nM ribosome, 80 nM mRNA, 25 °C. The other components of the translation reaction mixture are summarized in Table 2.

releases the nascent peptide chain.[35] Fusidic acid binds to EF-G to inhibit the peptide elongation process.[36] Kasugamycin binds to the 30S ribosomal subunit to inhibit the reassociation of the 50S subunit during translation initiation.[33,34]

Figure 3 shows the typical frequency changes that were obtained after the addition of 1 μM antibiotic to the translation reaction. When puromycin was injected during the translation reaction 15 min after the injection of the mRNA, the frequency increased (mass decreased) rapidly and reverted to the original value [curve (a)]. Since puromycin can bind to the A site of the ribosome and release the nascent peptide chain, the rapid increase in frequency could be explained by the release of the ribosome from the nascent peptide that was bound to the streptavidin on the QCM.

When fusidic acid was injected 15 min after the mRNA, the decrease in frequency was stopped almost completely [curve (b)]. The inhibition of peptide elongation by the binding of fusidic acid to EF-G could prevent the formation of additional RNCs. In other words, we could monitor the actual increase in concentration of RNCs as the frequency decreased.

Kasugamycin injected 15 min after the mRNA had very little effect on the change in frequency compared with that obtained in the absence of antibiotics [curve (c)]. In contrast, when kasugamycin was added prior to the injection of the mRNA, only a small decrease in frequency was observed [curve (d)]. These results indicate that kasugamycin inhibits the formation of the initiation complex but cannot inhibit translation once the initiation complex has been formed. These findings support the suggestion that the time lag after the addition of mRNA could correspond to the time required for the formation of the initiation complex and that the subsequent frequency decrease is due to the production of RNCs.

Table 3. Comparison of the Time Lags Obtained with Different Triggers and 5′-UTR Sequences[a]

		time lag (min)		
run	trigger	Enhancer-mRNA	Can-mRNA	Strong-mRNA
1	mRNA	8.7 ± 0.3	10.0 ± 0.2	10.7 ± 0.2
2	EF-Tu/GTP	8.5 ± 0.2	9.1 ± 0.2	9.4 ± 0.3
3	EF-G	6.9 ± 0.4	6.9 ± 0.3	7.1 ± 0.6

[a] Data show the time lags after the addition of the mRNA (Run 1, Figure 4), EF-Tu/GTP (Run 2, Figure 6A), and EF-G (Run 3, Figure 6B).

Effects of 5′-UTR Sequences on Translation. The 5′-UTR region of an mRNA is important for translation in bacteria, and ribosomes initiate translation by binding first to an SD sequence that is located immediately upstream of the start codon (AUG). The SD sequence is complementary to the 3′ end of 16S rRNA (the anti-SD sequence) in the 30S ribosomal subunit, and the correct degree of complementarity is important to allow translation initiation to occur.[37] Furthermore, it has been shown that the 5′-UTR, which is located upstream of the SD sequence, has a significant effect on the efficiency of protein synthesis. We prepared three mRNAs that contained different 5′-UTRs, as shown in Table 1: Can-mRNA contained only the canonical SD sequence (AAGGAG) and no enhancer sequence; Strong-mRNA had a higher degree of complementarity to the anti-SD sequence because it contained the sequence UAAGGAGGTGATC; and Enhancer-mRNA contained a translational enhancer from a T7 phage gene[5,6] located upstream of the SD sequence (UUAACUUUAAgAAGGAG).

Figure 4 shows the typical changes in frequency obtained after the addition of each mRNA to the translation mixture. The extent of the time lag and the rate of production of the SBP tag (i.e., the slope of the frequency decrease) were dependent on the 5′-UTR sequence used. The results are summarized in Table 3. Here the frequency changes were normalized to their own maximum frequency changes because the final amounts of

(35) Nathans, D. *Proc. Natl. Acad. Sci. U.S.A.* **1964**, *51*, 585–592.
(36) Cabrer, B.; Vázquez, D.; Modolell, J. *Proc. Natl. Acad. Sci. U.S.A.* **1972**, *69*, 733–736.
(37) Shine, D.; Dalgarno, L. *Proc. Natl. Acad. Sci. U.S.A.* **1974**, *71*, 1342–1346.

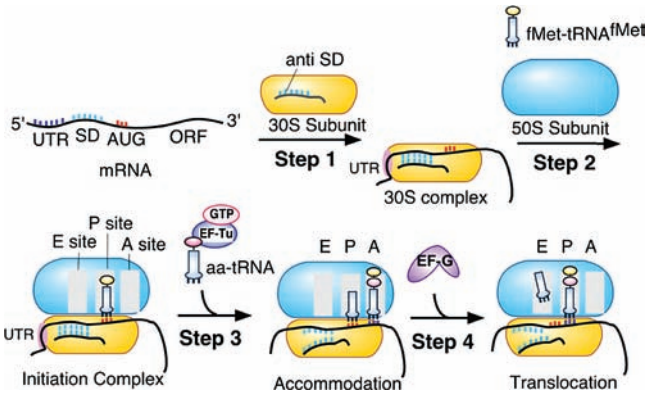

Figure 5. Schematic illustration of the initiation and elongation steps of translation. Step 1: the 30S ribosome binds to the SD sequence on mRNA via the interaction between the SD and anti-SD sequences. Step 2: the 50S ribosome and fMet−tRNA^{fMet} bind to the 30S ribosome and the mRNA to form the initiation complex. Step 3: EF-Tu delivers the aa-tRNA corresponding to the second codon to the A site. Step 4: EF-G catalyzes the translocation of the 70S ribosome to the next codon. The 5′-UTR sequence is presumed to interact with the 30S ribosome in the 30S complex and the initiation complex.

bound RNCs depended on the amounts of streptavidin bound on the QCM plate, which were in the range 2.6 ± 0.2 pmol. Enhancer-mRNA showed a shorter time lag (8.7 ± 3 min) and a steeper slope (0.04 Hz s^{-1}) than those obtained with the standard Can-mRNA (10.0 ± 0.2 min and 0.032 Hz s^{-1}, respectively). On the other hand, when Strong-mRNA was utilized, the time lag was longer (10.2 ± 0.2 min) and the slope gentler (0.021 Hz s^{-1}) than those observed with Can-mRNA.

Figure 5 shows a schematic illustration of the stages of translation. In step 1, the anti-SD sequence on the 30S ribosome interacts with the SD sequence on the mRNA. In step 2, the translation initiation complex is formed, and the initiator tRNA fMet−tRNA^{fMet} is introduced into the P site of the 70S ribosome. In step 3, an aminoacyl−tRNA (aa-tRNA) that is complementary to the second codon is delivered to the A site by EF-Tu/GTP. In step 4, the ribosome translocates along the mRNA to the next codon in a process that is catalyzed by EF-G (the P and A sites become E and P sites, respectively). The differences in the time lag resulting from the use of different 5′-UTRs indicate that the 5′-UTR may affect some of the rate-limiting steps in the primary translation process.

The PURE system allows the translation factors that are added to the reaction mixture to be adjusted easily. Therefore, it was highly advantageous to be able to combine the PURE system with the QCM technique in order to investigate the stepwise reactions of translation. When the QCM cell was filled with translation mixture that did not contain EF-Tu/GTP, virtually no decrease in frequency was observed after the mRNA was injected to trigger translation (the first arrow in Figure 6A). This means that translation could not proceed beyond step 2. The addition of EF-Tu/GTP after 20 min triggered a decrease in frequency with time lags of 8.5 ± 0.2, 9.1 ± 0.2, and 9.4 ± 0.3 min for Enhancer-mRNA, Can-mRNA, and Strong-mRNA, respectively. The time lags obtained are summarized in Table 3. The time lags obtained in Figure 6A (run 2 in Table 3) were shorter than those obtained when the mRNA was injected into the complete reaction mixture, shown in Figure 4 (run 1 in Table 3). Furthermore, the 5′-UTR-dependent differences in the time lag were smaller when translation was triggered by the addition of EF-Tu-GTP than when translation was triggered by the injection of mRNA alone. In the latter case, the time lag included

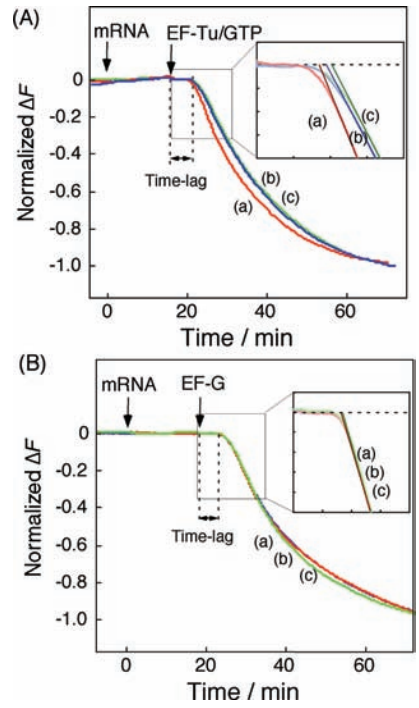

Figure 6. Effect of (A) EF-Tu/GTP and (B) EF-G triggers on the time lag before the start of translation in the presence of different 5′-UTR sequences: (a) Enhancer-mRNA, (b) Can-mRNA, and (c) Strong-mRNA. QCM cells were filled with translation mixture without mRNA and EF-Tu/GTP or EF-G, and translation was started by the addition of mRNA and then EF-Tu/GTP or EF-G. Conditions: 50 mM HEPES buffer (pH 7.6), 40 nM ribosomes, 80 nM mRNA, 25 °C. The other components of the translation reaction mixture are summarized in Table 2.

all four steps of the translation process. In contrast, when the translation was triggered by EF-Tu/GTP, only steps 3 and 4 contributed to the time lag.

When the QCM cell was filled with translation mixture that did not contain EF-G and mRNA was injected, translation could not proceed beyond step 3 (Figure 5). The addition of EF-G after 20 min triggered a decrease in frequency with a time lag of 7.0 min, which was independent of the 5′-UTR sequence (Figure 6B and run 3 in Table 3) and shorter than those observed when translation was triggered by mRNA (run 1) or EF-Tu/GTP (run 2). Therefore, the 5′-UTR does not affect step 4. In other words, during step 4, the 30S ribosome may no longer interact with the 5′-UTR, as shown schematically in Figure 5. The observation that the time lag triggered by EF-G is shorter than those triggered by mRNA and EF-Tu/GTP indicated that step 4 was not strongly rate-limiting. As shown in Table 3, the time lags between the addition of the trigger and the start of translation decreased in the order mRNA > EF-Tu/GTP > EF-G. The effect of the 5′-UTR sequence on the time lag when the different triggers were used decreased similarly in the order mRNA > EF-Tu/GTP > EF-G. Since the time lags triggered by mRNA, EF-Tu/GTP, and EF-G represent steps 1−4, step 3, and step 4 of translation, respectively, the results suggest that the 5′-UTR strongly affects the formation of the initiation complex (steps 1 and 2) through the interaction with the 30S ribosome and also affects the accommodation of the second aa-RNA into the A site by EF-Tu/GTP (step 3).

Mechanism of Efficient Translation. In bacteria, the ribosome has two different modes of interaction with the mRNA. The first involves specific binding of the ribosome to the SD sequence on the mRNA to initiate the translation reaction, and

the other involves linear scanning along the mRNA to translate the ORF that lies downstream of the SD sequence. Thus, when the SD and anti-SD sequences dissociate from each other, the ribosome can start to scan along the downstream ORF. The mRNA-triggered experiments showed that the length of the time lag depended on the degree of complementarity between the SD and anti-SD sequences (Strong-mRNA > Can-mRNA; see Table 2). These results indicated that the strong SD−anti-SD interaction that occurred within the initiation complex prevented the smooth transition from translation initiation to elongation. On the other hand, since the enhancer sequence shortened the time lag, it is possible that the translational enhancer weakened the formed SD−anti-SD duplex. It has also been reported that the amount of translation decreases in the presence of a strong SD sequence, but the translational enhancer restores translation in spite of its high complementarity to the 16S rRNA.[7] Therefore, we propose that the 5′-UTR controls the free-energy barrier (within step 2 to 3 and step 3 to 4) from translation initiation to translation elongation, which in turn determines the efficiency of translation.

Recent structural studies may help to explain the mechanism by which the 5′-UTR affects the efficiency of both the formation of the initiation complex and the accommodation of the second aa-tRNA in the A site. It has been proposed that movement of the SD duplex is involved in the transformation of the initiation complex into the postinitiation complex (peptide-elongation complex) and that the second aa-tRNA binds to the postinitiation complex rather than the initiation complex.[38−40] Single-molecule analysis also revealed that the SD−anti-SD interaction is weakened during the accommodation of the second aa-tRNA.[41] Thus, because the stability of the SD duplex depends on the complementarity of the SD sequence to the 16S rRNA, the efficiency of translation initiation could be controlled by the sequence upstream of the start codon. In contrast, it is suggested that the translational enhancer interacts with ribosomal protein S1.[7] We predict that the interaction between the translational enhancer and S1 destabilizes the SD duplex allosterically and promotes an efficient transition from the initiation phase to elongation.

Conclusion

We have reported the novel application of the QCM technique to the observation of a single-turnover reaction of protein synthesis in real time with no requirement for labeling. The combination of QCM and a reconstituted cell-free translation system permitted the detection of the newly synthesized protein with quite high sensitivity and the evaluation of different antibiotics and analysis of the mechanism of translational regulation by the 5′-UTR. Our findings suggest that the mRNA sequence itself could control the efficiencies of the translation reaction. With this methodology, the effects of sequences such as UTRs and ORFs on protein synthesis and protein folding can be analyzed by simply measuring a change in mass.

JA9019947

(38) Yusupov, M. M.; Yusupova, G. Z.; Baucom, A.; Lieberman, K.; Earnest, T. N.; Cate, J. H. D.; Noller, H. F. *Science* **2001**, *292*, 883–896.
(39) Jenner, L.; Romby, P.; Rees, B.; Schulze-Briese, C.; Springer, M.; Ehresmann, C.; Ehresmann, B.; Moras, D.; Yusupova, G.; Yusupov, M. *Science* **2005**, *308*, 120–123.
(40) Yusupova, G.; Jenner, L.; Rees, B.; Moras, D.; Yusupov, M. *Nature* **2006**, *444*, 391–394.
(41) Uemura, S.; Dorywalska, M.; Lee, T. H.; Kim, H. D.; Puglisi, J. D.; Chu, S. *Nature* **2007**, *446*, 454–457.